

Supporting Information

Chiral One-dimensional O-P-O bridged Mn^{III}-Schiff base complexes

Ting-Ting Wang, Song-Song Bao*, Jian Huang, Yi-Zhi Li, Li-Min Zheng*

State Key Laboratory of Coordination Chemistry, Coordination Chemistry Institute, School of Chemistry and Chemical Engineering,
Nanjing University, Nanjing 210093, P. R. China; E-mail: lmzheng@nju.edu.cn, baososo@nju.edu.cn

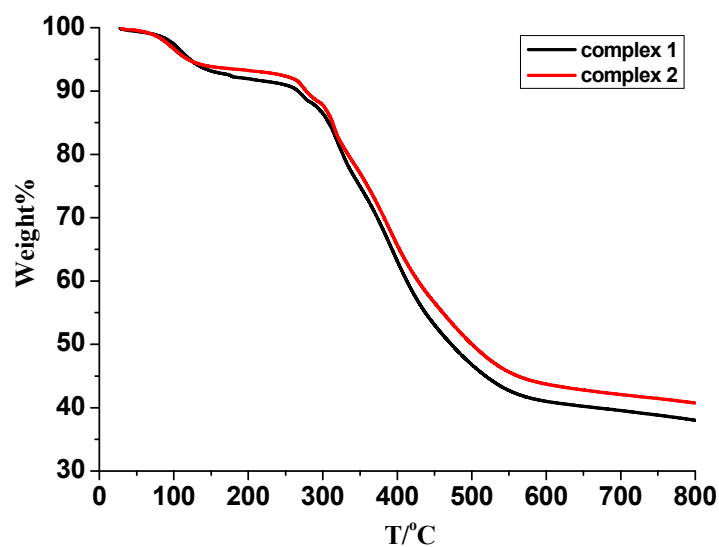


Figure S1. The TG curves of 1 and 2.

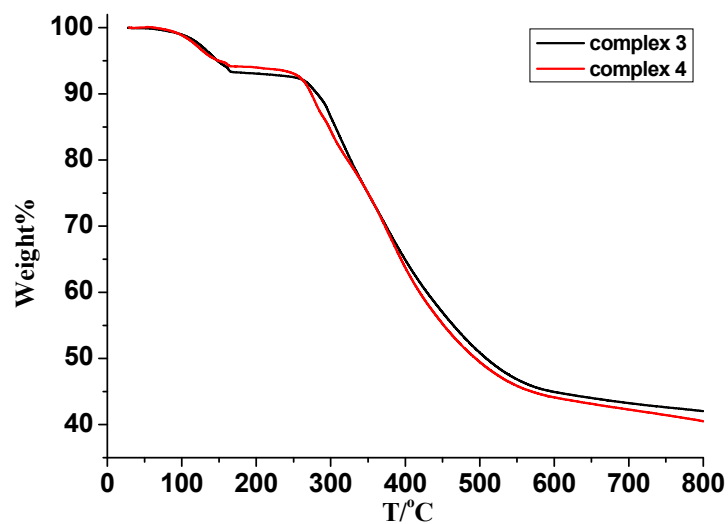


Figure S2. The TG curves of 3 and 4.

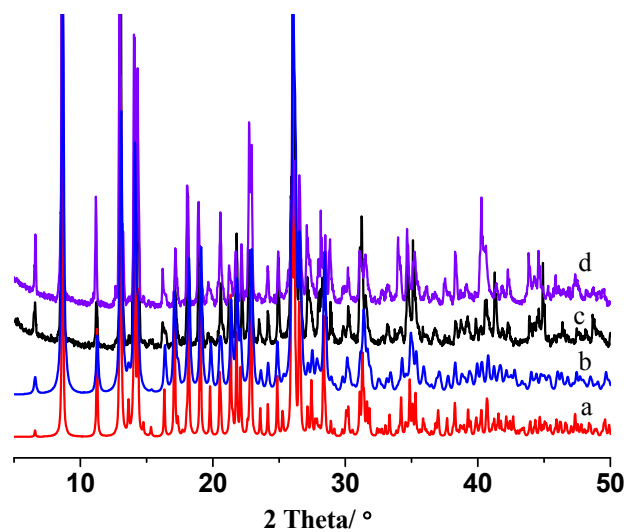


Figure S3. Powder X-ray diffraction patterns for **1-2**: (a) simulated from single-crystal data of **1**, (b) simulated from single-crystal data of **2**, (c) bulk sample of **1**, (d) bulk sample of **2**.

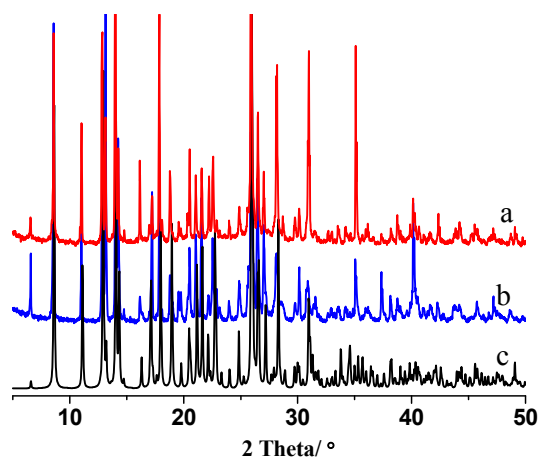


Figure S4. Powder X-ray diffraction patterns for **3-4**: (a) simulated from single-crystal data of **3**, (b) bulk sample of **4**, (c) bulk sample of **3**.

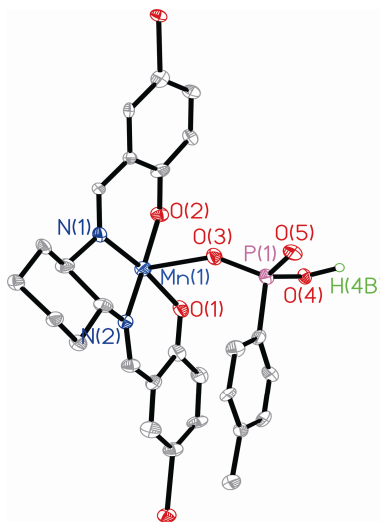


Figure S5. Structural unit of **3** showing the atomic labeling scheme (30% probability). All hydrogen atoms except those attached to the oxygen atoms are omitted for clarity.

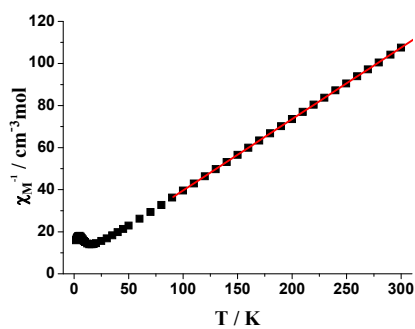


Figure S6. Plot of the $1/\chi_M$ versus T for **1**. The red solid line represents the best fit of the data above 100 K.

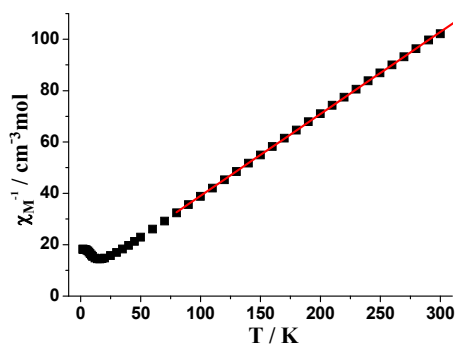


Figure S7. Plot of the $1/\chi_M$ versus T for **3**. The red solid line representd the best fit of the data above 100 K.

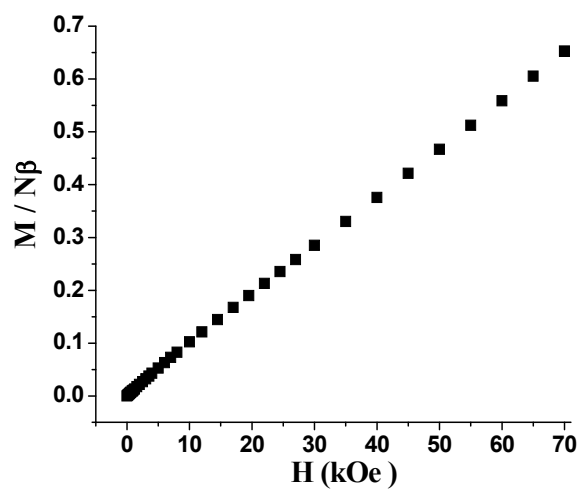


Figure S8. Field-dependent magnetization of **1** at 2 K.

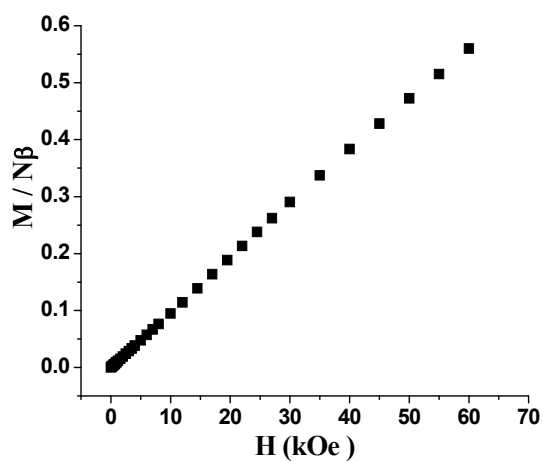


Figure S9. Field-dependent magnetization of **3** at 2 K.

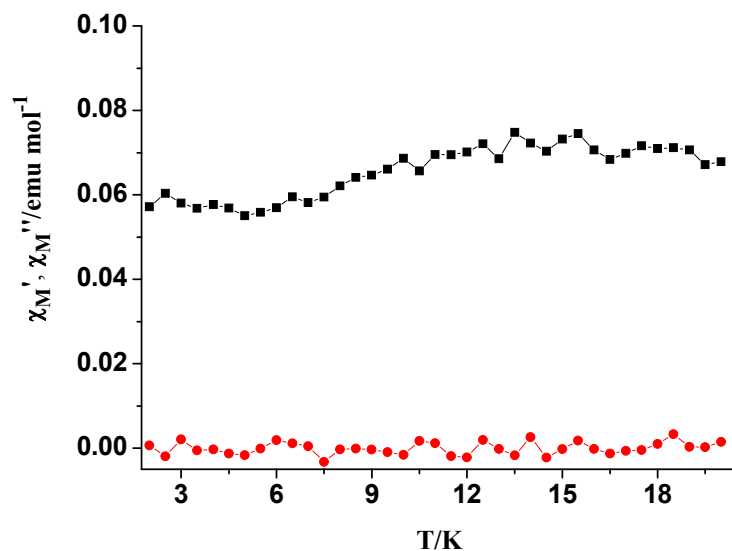


Figure S10. Plots of in-phase (χ_M' , black) and out-of-phase (χ_M'' , red) ac magnetic susceptibility versus T at 1 Hz for **1**.

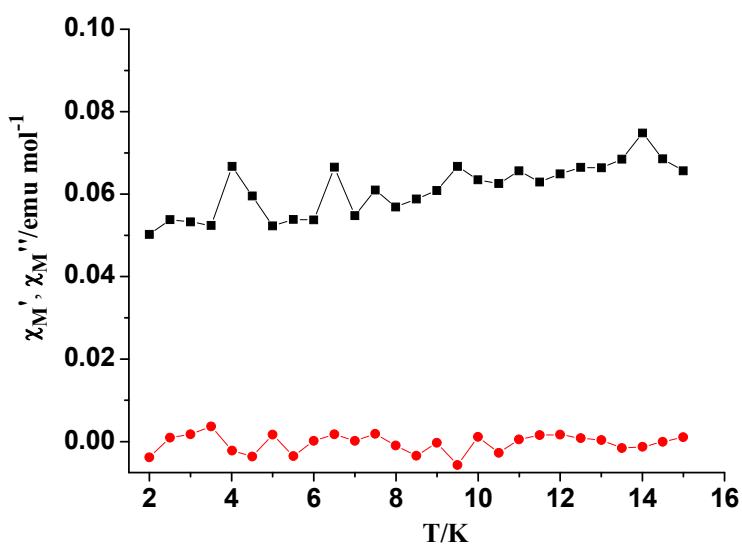


Figure S11. Plots of in-phase (χ_M' , black) and out-of-phase (χ_M'' , red) ac magnetic susceptibility versus T at 1 Hz for **3**.